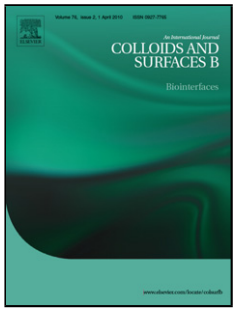

Title: Membrane Surface Functionalization via Theophylline Derivative Coating and Streptavidin Immobilization

Author: J. Hierrezuelo V. Romero J. Benavente R. Rico J. Manuel López-Romero

PII: S0927-7765(13)00574-2
DOI: http://dx.doi.org/doi:10.1016/j.colsurfb.2013.09.007
Reference: COLSUB 6007

To appear in: *Colloids and Surfaces B: Biointerfaces*

Received date: 6-5-2013
Revised date: 5-8-2013
Accepted date: 3-9-2013

Please cite this article as: J. Hierrezuelo, V. Romero, J. Benavente, R. Rico, J.M. López-Romero, Membrane Surface Functionalization via Theophylline Derivative Coating and Streptavidin Immobilization, *Colloids and Surfaces B: Biointerfaces* (2013), http://dx.doi.org/10.1016/j.colsurfb.2013.09.007

Membrane Surface Functionalization *via* Theophylline Derivative Coating and Streptavidin Immobilization

J. Hierrezuelo,[1] V. Romero,[2] J. Benavente,[2] R. Rico,[1] J. Manuel López-Romero[1]*

[1]Dep. de Química Orgánica, [2]Dep. de Física Aplicada I
Facultad de Ciencias, Universidad de Málaga, E-29071 Málaga, Spain
jmromero@uma.es

Abstract

Poly(vinylidene fluoride) (PVDF) and regenerated cellulose (RC) membranes were surface–modified by the adsorption of one adenosine receptor antagonist: the theophylline–oligo(ethylene glycol)–alkene derivative, Theo**1**. Surface modification was carried out by immersion of the membrane in a dichloromethane solution of Theo**1** (PVDF+Theo**1** and RC+Theo**1** samples). Membrane surfaces with partial coverage by theophylline and/or its inclusion in the membrane structures were studied by X–ray photoelectron spectroscopy (XPS), solid–state nuclear magnetic resonance (SNMR), impedance spectroscopy (IS) and contact angle (CA) measurements. The Theo**1** orientation was inferred from the data. Streptavidin (SA) was immobilized onto the membrane/Theo**1** hybrid material. The protein–theophylline Theo**1** interaction was visualized with bright field microscopy (BFM).

Key words: membrane modification, theophylline, physicochemical characterization, biosensor

1. Introduction

The modification of solid substrates, including membranes, using bioactive materials is an attractive field of research for developing new devices such as biosensors, structured multilayers or controlled-release delivery systems [1-3]. Membrane grafting, atomic layer deposition, photolithography and deep coating are typical surface modification techniques depending on membrane materials and specific applications [4-7]. Particularly, this later technique is an easy way of membrane modification without involving chemical reactions. Among other materials, regenerated cellulose (RC) and poly(vinylidene fluoride) (PVDF) membranes are commonly used since they present good chemical resistance and thermal stability. PVDF porous membranes have biomedical applications such as hemodialysis, hemapheresis or protein filtration [8,9]. RC membranes are commonly used in different membrane separation processes. Particularly, cellulose has been employed in the manufacture of dialysis membranes due to their high hydrophilicity [10]. Cellulose membranes have been biofunctionalized by carboxybetaines for improving blood compatibility [11] or by chimeric avidin [12] to be used as sensor with even single molecule sensitivity [13]. The chemical nature of both types of membranes renders them excellent support materials for biotechnological and medical applications [14].

On the other hand, theophyllines are methylxantine derivatives with pharmacological applications and they have been used as templates in molecularly imprinting polymers (MIPs) related research [15]. The biological effect of theophyllines is associated to its affinity with a family of adenosine receptors known as A_1, A_{2A}, A_{2B}, and A_3 [16]. Recently, several 1,3-dialkyl deazaxanthines as well as several theophylline-oligo(ethylene glycol) based anchors have been reported as potent A_{2B} adenosine receptor antagonists [17,18]. In particular, the oligo(ethylene glycol)–alkene theophylline substituted (Theo**1**, Fig. 1) exhibited one of the highest affinity for human A_{2B} receptor (Ki = 4.16 nM) with a selectivity Ki_{A2A}/Ki_{A2B} of 24.1 and a solubility in

water of 1 mM. Besides, through the binding with the above adenosine receptors, theophylline derivatives are well known to influence neuronal activities [19].

Fig. 1. A_{2B} antagonist active theophylline–oligo(ethylene glycol)–alkene derivative (Theo**1**)

Particularly, the affinity of Theo**1** for adenosine receptors is close to the affinity of extensively studied biotin for streptavidine (around *Ki* = 100 fM), one of the strongest receptor-ligand interactions found in nature. The exceptionally high affinity of the biotin-SA pair has made it extremely useful for many biotechnological applications, such as affinity separations, diagnostic assays biomolecular imaging, anticancer therapies and the delivery of therapeutics [20]. The high affinity found for the system adenosine receptor–Theo**1** opens the possibility of using this pair for the analysis of SA interactions.

One of the points of interest in our research is the inclusion/immobilization of pharmacologically active molecules on solid substrates and the study of their interactions with permeable solutes [21,22]. Particularly, in this paper we present the results on functionalization of membrane surfaces with compound Theo**1** and its interaction with Atto-565-streptavidin conjugate, a biotin–binding protein. We have selected two support membranes from different materials (hydrophilic regenerated cellulose and hydrophobic PVDF) and structures (porous PVDF and dense or swollen RC membranes) in order to also obtain information on the effect of these factors on the membrane functionalization. Theo**1** films on the membrane surfaces have been characterized by SNMR, XPS and IS, which allows us the estimation of modifications in electrical parameters for both bulk–membrane and membrane–surface/electrode. Moreover, changes in the hydrophilic character of membranes surfaces obtained by contact angle measurements gives information on the orientation of Theo**1** active on the surfaces of both

membranes. Furthermore, bright field microscopy (BFM) was used to visualize the SA protein interaction with the surface of both modified membranes.

2. Experimental

2.1. Materials and reagents

Compound Theo**1** was prepared by following the procedure previously developed in Ref. [18]. Atto-565-streptavidin (# 56304) was purchased from Fluka (Madrid, Spain).

Two flat supports with different characteristics, a highly hydrophilic dense cellophane film (RC) from Cellophane Española S. A. (Burgos, Spain) and a porous PVDF membrane with 0.02 μm pore size from Pall (Versapore® w/wa, Michigan, USA), were selected.

*2.2. Membrane modification with compound Theo**1***

Adsorption of Theo**1** onto the surfaces of the selected membrane supports (RC and PVDF) was carried out by immersion of a piece of the membrane (1 cm x 0.3 cm) in a dichloromethane solution of Theo**1** (1 mM). The system was slowly stirred for half an hour at room temperature (25 ºC). The membranes were then removed, washed with dichloromethane and dried at room temperature in a desiccator for 24 h, to obtain the modified samples that will hereafter be referred as RC+Theo**1** and PVDF+Theo**1**.

2.3. Membrane streptavidin immobilization procedure

A diluted solution (1 mL, 1 ng/μL) of streptavidin (SA) in PBS was prepared from the concentrated commercial streptavidin solution (667 ng/μL). This solution was kept in cold (5 ºC) and protected from light. Then, in two vials of 2 mL volume each, two pieces (1 cm x 0.3 cm) of

pristine and Theo**1**–modified support membranes (RC and RC+Theo**1**; PVDF and PVDF+Theo**1**) were immersed in the streptavidin solution (0.5 mL); the solution was slowly stirred and protected from light at room temperature for 30 min. After this period, membranes were washed with cold water and dried over a Whatman 3MM paper in a desiccator. Once they were dried (*c.a.* 12 h) they were kept in cold. Streptavidin functionalized samples will hereafter referred as RC+Theo**1**+SA and PVDF+Theo**1**+SA. Analysis by UV of SA residual solution showed a very low protein concentration.

2.4. Membrane characterization by XPS, CA, SNMR, IS and BFM

XPS analysis was carried out using a Physical Electronics PHI ESCA 5701 spectrometer with a non-monochromatic Mg Kα radiation (300 W, 15 kV, 1253.6 eV) as the excitation source. High–resolution spectra were recorded in the constant pass energy mode at 29.35 eV, using a 720 μm diameter analysis area and the pressure in the analysis chamber was maintained lower than 5 10^{-6} Pa. PHI ACCESS ESCA-V6.0 F software package was used for acquisition and data analysis. Curve fitting was performed using the software supplied by the manufacturer. Atomic concentration percentages of the characteristic elements on the membranes surfaces were determined taking into account the corresponding area sensitivity factor for the different measured spectral regions [23,24]. Membrane samples were irradiated for a maximum time of 20 min to minimize possible X-ray damage [25].

Changes in the hydrophilic character of the membranes surfaces associated to compound Theo**1** deposition were determined from contact angle (CA) measurements, which were performed with a Teclis T2010 instrument equipped with a video system. Six measurements on both surfaces of each membrane were taken.

^{1}H and ^{13}C SNMR spectra were recorded with a Varian NMR (U.K.) system NB500 operating at 500 MHz. Spectrometer was equipped with a FastMAS 1.6 mm HXY probe. Analyses were carried out for the PVDF+Theo**1** sample.

Impedance spectroscopy measurements with dry samples of pristine and Theo**1**–modified membranes were performed with a Frequency Response Analyzer (Solartron 1260, England) and taken 100 data points for frequency ranging between 1 Hz and 10^7 Hz, at a maximum voltage of 0.01 V. The test cell consists of a Teflon support on which two Pt electrodes were placed and screwed down.

Optical transmission microscopy (bright field, BFM) was used to visualize the interaction of Theo**1**–modified membranes (RC+Theo**1**+SA and PVDF+Theo**1**+SA samples) with the protein. Images were obtained with a Leika TCS SP5 system (Madrid, Spain), which allows deep imaging analysis.

3. Results and discussion

The presence of compound Theo**1** adsorbed onto the surfaces of PVDF and RC membranes was study by XPS and solid–state NMR as well as impedance spectroscopy and contact angle measurements.

Surfaces of pristine (PVDF and RC) and theophylline treated (PVDF+Theo**1** and RC+Theo**1**) membranes were chemically characterized by XPS measurements. XPS spectra give information on the chemical states of the elements present on the membrane surfaces and their atomic concentration percentages (A.C. %). Fig. 2 shows a comparison of C 1s core level spectra recorded for pristine and treated membranes where different contributions representing the various bonding environments can be observed. Fig. 2(a) shows two clear peaks for the PVDF support which are ascribed to the $–CF_2–$ bond (C_A peak at 291.0 eV) and to the $–CH_2–$ bond (C_C

peak at 286.7 eV), while for the PVDF+Theo**1** sample the contribution of the –C-N– bonds at 286.3 eV can also be observed; moreover, a significant shoulder associated to the –C-C– bonds (C_B at 285.0 eV) and another smaller at 288.0 eV (C_D) due to –C=O– bonds can also be distinguished [26,27]. In the case of the cellulosic RC+Theo**1** membrane, the C 1s core level spectra shows a reduction in the peak corresponding to the aliphatic carbon (C_A) as well as the contribution of the –C-O– and –C-N– bonds (C_C) [24,25].

Fig. 2. C 1s core level spectra for pristine (dashed lines) and theophylline **1** treated (solid lines) membranes: (a) PVDF; (b) RC

Table 1 shows the average values of the different elements found on both membrane surfaces. Since the polyvinylidene fluoride PVDF membrane only contains carbon and fluorine in its structure ($[CH_2CF_2]_n$), the small percentage of oxygen is attributed to impurities associated to contamination (entry 1) [23], which are also responsible for the small nitrogen percentage detected in cellulosic RC membrane (entry 3). With respect to the characteristic elements of each membrane (carbon and fluorine for the PVDF, carbon and oxygen for the RC), there was a significant reduction of fluorine (%) on the PVDF+Theo**1** sample and an increase in oxygen and nitrogen percentages (entry 2), indicating the presence of Theo**1** on the surface of the modified membrane. A similar effect is also observed for the RC+Theo**1** membrane (entry 4) by considering the increase in the nitrogen and the reduction in the oxygen percentages. These results show the partial coverage of the surfaces of both membranes by Theo**1** in agreement with published results [26].

Table 1. Average atomic concentration percentages* of the different elements present on the surface of pristine and Theo**1** treated PVDF and RC membranes.

Entry	**Membrane**	**C 1s** (%)	**O 1s** (%)	**F 1s** (%)	**N 1s** (%)
1	PVDF	52.5 ± 0.4	1.9 ± 0.5	45.6 ± 1.2	-----
2	PVDF+Theo**1**	64.2 ± 0.8	11.4 ± 0.6	19.7 ± 1.2	4.7 ± 0.6
3	RC	61.9 ± 0.9	37.9 ± 0.6	-----	0.2 ± 0.1
4	RC+Theo**1**	75.1 ± 0.4	17.6 ± 0.2	-----	7.3 ± 0.1

*Average values and error intervals (standard deviations) correspond to measurements at both membrane surfaces.

The presence of theophylline Theo**1** in the PVDF support was also studied by solid–state NMR. The ^{1}H SNMR (Fig. 3(a)) did not have enough resolution to resolve the overlapped signals around 3 ppm, which is a common situation in solid–state NMR since broadening of the spectral lines reach to a few ppm (2–5 ppm). However, in ^{13}C SNMR spectrum (Fig. 3(b)), theophylline signals can be clearly seen and do fit the lines for the theophylline derivative Theo**1**. By comparison with the reported data [18], picks at 158.9, 153.9, 151.0, 148.8 and 147.6 ppm can be assigned to the quaternary carbon atoms and C=N, C-4, C=O and C=O carbon atoms, respectively. Signal at 106.3 ppm can be attributed to the C-5 of the theophylline moiety. In the aliphatic part of the spectrum, signals corresponding to the methylene groups of the ethylene glycol moiety appears at 70.9 and 66.0 ppm, while N-Me groups and $–CH_2–$ are observed at 30.4, 28.3 and 21.2 ppm. On the other hand, the two major lines at 120.9 ppm and 42.8 ppm are from PVDF ($–CF_2–$ and $–CH_2–$ resonances, respectively) [28,29], and they are also broad which typical for NMR in solids.

Fig. 3. Solid–state ^{1}H SNMR (left) and ^{13}C SNMR (right) of Theo**1** modified PVDF membrane

Impedance spectroscopy plots also confirm the presence of Theo**1** in the surfaces of both modified membranes as well as in the structure of the swollen RC support. Fig. 4 shows a comparison of the impedance curves obtained for pristine and Theo**1**–modified membranes. Significant differences for both membrane/electrode interface and bulk membrane can be observed, being an indication of the membrane surface coverage by theophylline Theo**1** and its inclusion into the cellulosic chains (Fig. 4(a)). Only membrane/electrode interface differences seem mainly to exist in the case of the PVDF sample (Fig. 4(b)) indicating a surface coverage without (or minor) theophylline Theo**1** inclusion into the pores of this support membrane [30].

Fig. 4. Impedance plots for dry samples of: (a) RC (o) and RC+Theo**1** (●) membranes; (b) PVDF (□) and PVDF+Theo**1** (■) membranes

Contact angle (ϕ) is the common measure for the characterization of hydrophobic/hydrophilic character of surfaces. Changes in membrane–surface/water contact angle as a result of theophylline Theo**1** partial coverage were also determined, and their average values $\langle\phi\rangle$ are indicated in Table 2. As can be observed, the presence of Theo**1** on the supports increases the hydrophobic character of both RC and PVDF membranes. This fact can be attributed to the attachment of the Theo**1** to the supports through the oligo(ethylene glycol)–alkene chain (see Fig. 5); it means an exterior orientation of the apolar moiety of the molecule (theophylline rest) with respect to the surface. As expected, this effect is stronger for RC due to the high hydrophilic character of this membrane (significantly higher than that of PVDF), which favors the interaction of hydrophilic part (OEG) of Theo**1** with the membrane. These results also agree with the found interfacial effects, which were previously indicated by analyzing the impedance plots.

Table 2. Average contact angle values <ϕ>* for pristine and theophylline Theo**1** treated membranes.

Membrane	**RC**	**RC+Theo1**	**PVDF**	**PVDF+Theo1**
<ϕ> (º)	35 ± 5	64 ± 8	82 ± 2	120 ± 9

*Average values and error intervals (standard deviations) correspond to six different measurements.

The possible self–attachments of Theo**1** on membranes and subsequent streptavidin immobilization are schematically described in Fig. 5. XPS data show a partial coverage of the membrane surface and an irregular distribution of Theo**1** on the surface can be expected.

Fig. 5. The scheme of the modification of the membrane surface with Theo**1** and then streptavidin immobilization

As was already indicated, pieces of Theo**1**–modified membranes were immersed in a solution of Atto-565-streptavidin in aqueous buffer PBS (samples RC+Theo**1**+SA and PVDF+Theo**1**+SA) in order to determine Theo**1**–protein interaction by bright field confocal images. First, Figs. 6(a) and 6(d) show the images of RC and PVDF supports treated with protein solution. No interaction between the protein and the surface of the membranes seems to exist since the characteristic red color of the Atto chromophore was not observed. Figs. 6(b) and 6(e) correspond to both Theo**1**–modified membranes (RC+Theo**1** and PVDF+Theo**1** samples, respectively): as expected no coloration by BFM was observed. However, for RC+Theo**1**+SA and PVDF+Theo**1**+SA samples (Figs. 6(c) and 6(f)) the red coloration of their surfaces was clearly observed, meaning the attachment of the protein on both membranes. In this sense, we assume a practically total SA immobilization according to the significant decrease of UV residual solution absorption with respect to the original one. Moreover, the random distribution of the red spots confirm the partial

coverage of the theophylline derivative on the surfaces as previously determined from XPS results, while BFM micrographs also confirm the Theo**1** orientation on the surfaces of both modified membranes as was obtained by CA results.

Fig. 6. Above: RC membrane surface having Theo**1** but non-treated with protein (a). RC surface without Theo**1** and treated with protein: no protein immobilization was observed (b). RC surface with **1** and treated with protein (RC+Theo**1**+SA, c). Below: PVDF membrane surface having Theo**1** (PVDF+Theo**1**) but non-treated with protein (d). PVDF surface without Theo**1** and treated with protein: no protein immobilization was observed (e). PVDF surface with Theo**1** and treated with protein ((PVDF+Theo**1**+SA, f).

4. Conclusion

This paper reports the deposition and/or inclusion of the theophylline derivative Theo**1** on the surface of porous and dense support membranes independently of the hydrophilic/hydrophobic character of the selected support. Theo**1** modification of pristine supports was established by different physicochemical characterization techniques, which could independently be used in further research: from the XPS and SNMR data we established the presence of Theo**1** on the membranes surface, and this point was confirmed by IS measurements. Moreover, CA technique provides information on the orientation of the Theo**1** active on the surface, indicating that most of this derivative is attached to the supports by the OEG chain.

Additionally, bright field microscopy probes the interaction of the fluorophore–labeled protein streptavidin with the modified membrane surface. This technique has allowed us to visualize the immobilization of SA on both Theo**1**–modified membranes and the significant capability of theophylline Theo**1** for SA binding.

Acknowledgements

We thank the financial support to CICYT (Spanish Projects CTQ/2010–17633 and CTQ/2011–27770, FEDER funds). V. Romero also thanks to CICYT for her FPU grant.

References

[1] C.M. Niemeyer, C.A. Mirking, Nanobiotechnology, Wiley–VCH, Weinheim, 2004.

[2] D.S. Goodsell, Bionanotechnology, Wiley–Liss, New Jersey, 2004.

[3] V. Kochev, M. Karabaliev, Adv. Colloid Interface Sci. 107 (2004) 9.

[4] B. Bhushan, Springer handbook on nanotechnology, Springer, New York, 2003.

[5] V. Romero, V. Vega, J. García, R. Zierold, K. Nielsch, V.M. Prida, B. Hernando, J. Benavente, ACS Appl. Mater. Interfaces, 5 (2013) 3556.

[6] S. Marchesan, C.D. Easton, K.E. Styan, P. Leech, T.R. GengenbachJ.S. Forsythe, P.G. Hartley, Colloids & Surf. B: Biointerfaces 108 (2013) 313.

[7] P. Alves, S. Pinto, J.-P. Kaiser, A. Bruinink, H.C. de Sousa, M.H. Gil, Colloids & Surf. B: Biointerfaces 82 (2011) 371.

[8] G. Laroche, Y. Marois, R. Guidoin, M.W. King, L. Martin, T. How, Y. Douville, J. Biomed. Mater. Res. 29 (1995) 1525.

[9] J.F. Hester, P. Banerjee, A.M. Mayes, Macromolecules 32 (1999) 1643.

[10] M. Mulder, Basic principles of membrane technology, Kluwer Academic Publishers, Dordrecht, 1992.

[11] M. Wang, J. Yuang, X. Huang, X. Cai, L. Li, J. Shen, Colloids & Surf. B: Biointerfaces 103 (2013) 52.

[12] J.J. Heikkinen, T.A. Riihimäki, J.A.E. Mättää, S.E. Suomela, J. Kantomaa, M.S. Kulomaa, V.P. Hytönen, O.E.O. Hormi, Appl. Matter. Interfaces 3 (2011) 2240.

[13] S. Jung, B. Angerer, F. Löscher, S. Niehren, J. Winkle, S. Seeger, ChemBioChem 7 (2006) 900.

[14] K. Sakai, J. Membr. Sci. 96 (1994) 91.

[15] M. Zacchigna, G. Di Luca, F. Cateni, V. Maurich, M. Ballico, G.M. Bonora, S. Drioli, Eur. J. Pharm. Sci. 30 (2007) 343.

[16] M. Legraverend, D.S. Grierson, Bioorg. Med. Chem. 14 (2006) 3987.

[17] A. Stefanachi, O. Nicolotti, F. Leonetti, S. Cellamare, F. Campagna, M.I. Loza, J. Brea, F. Mazza, E. Gavuzo, A. Carotti, Bioorg. Med. Chem. 16 (2008) 9780.

[18] J. Hierrezuelo, J.M. López–Romero, R. Rico, J. Brea, M.I. Loza, C. Cai, M. Algarra, Bioorg. Med. Chem. 18 (2010) 2081.

[19] J.A. Ribeiro, A.M. Sebastião, A. Mendonça, Prog. Neurobiol. 68 (2003) 377.

[20] S.L. Hisey, B.R. Peterson, J. Am. Chem. Soc. 124 (2002) 6265, and references there in.

[21] M.I. Vázquez, L. Peláez, J. Benavente, J. Hierrezuelo, R Rico, J.M. López–Romero, E. Guillén, M.R. López–Ramírez, J. Pharm. Sci. 100 (2011) 4815.

[22] J. Benavente, M.I. Vázquez, J. Hierrezuelo, R. Rico, J.M. López–Romero, M.R. López–Ramírez, J. Membr. Sci. 355 (2010) 45.

[23] J.F. Moulder, W.F. Stickle, P.E. Sobol, K.D. Bomben, Handbook of X-Ray Photoelectron Spectroscopy. J. Chastain Ed., Perkin-Elmer Corporation, Minneapolis, 1992.

[24] D. Briggs, M.P. Seah, Practical Surface Analysis, 2nd ed. Vol I: Auger and X-ray photoelectron spectroscopy, John Wiley & Sons, Chichester, 1995.

[25] M.J. Ariza, J. Benavente, E. Rodríguez-Castellón, The capability of X-ray Photoelectron Spectroscopy in the characterization of membranes: correlation between surface chemical and transport properties in polymeric membranes, *in* X-ray Photoelectron Spectroscopy, Nova Publishers, 2009, 257.

[26] L.P. Zhu, J.Z. Yu, Y.Y. Xu, Z.Y. Xi, B.K. Zhu, Colloids & Surf. B: Biointerfaces 69 (2009) 152.

[27] R. Fortunato, C.A.M. Afonso, J. Benavente, E. Rodriguez-Castellón, J.G. Crespo, J. Membr. Sci. 256 (2005) 216.

[28] S. Ando, R.K. Harris, and S.A. Reisnberg, Magn. Reson. Chem. 40 (2002) 97.

[29] T.W. Su, D.L.M. Tzou, Polymer, 41 (2000) 7289.

[30] J. Benavente, Use of impedance spectroscopy for characterization of membranes and the effect of different modifications, in Membrane Modification: Technology and Applications. Eds. N. Hilal, M. Khayet, C.J. Wright. CRC Press, 2012.

Highlights:

Modification of membrane surfaces by using bioactive materials
Theophylline derivative as an alternative to biotin for monitoring streptavidin interaction
Easy procedure for monitorization of the protein interaction by bright field microscopy

Figure(s)

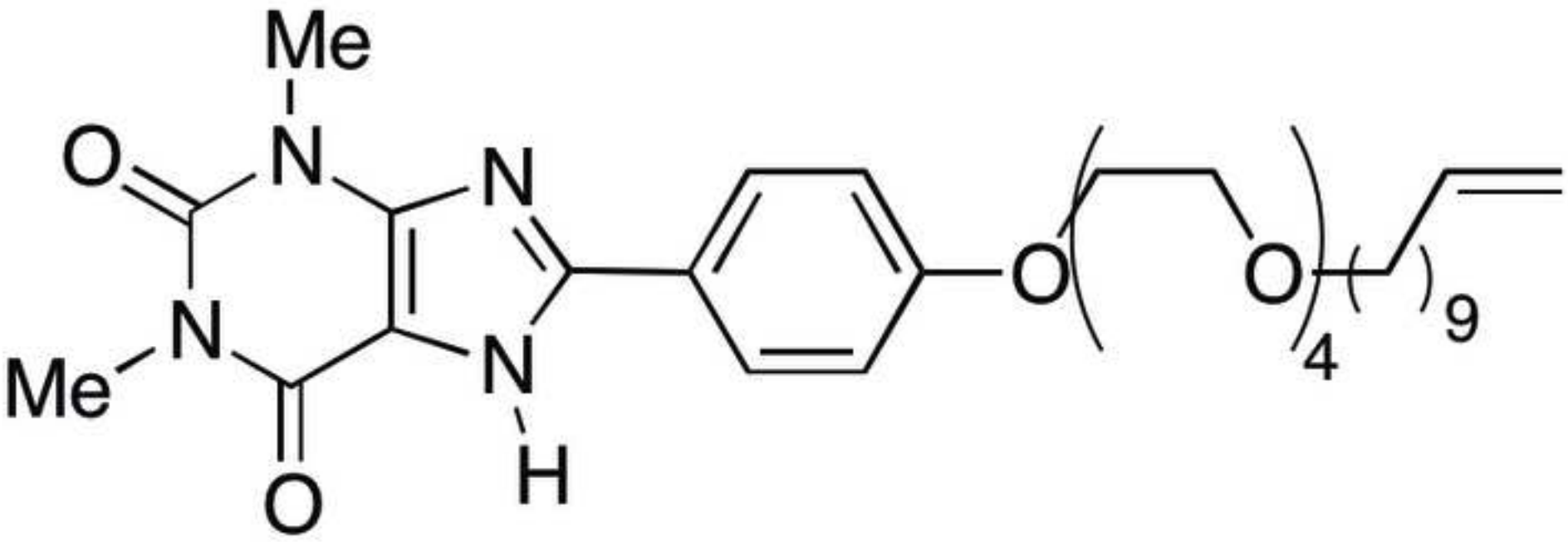

Theo**1**

Figure(s)

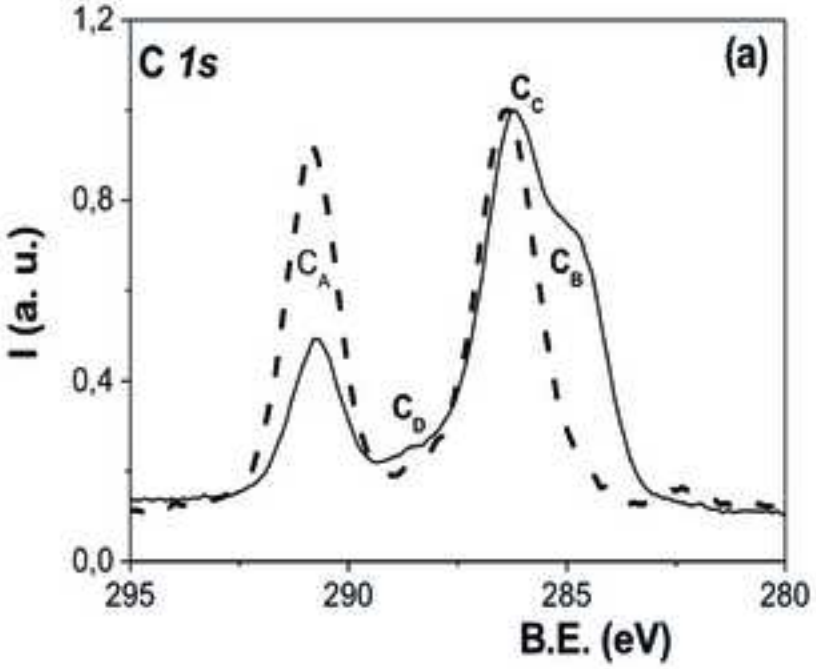
C 1s
(a)
I (a. u.)
1,2
0,8
0,4
0,0
295
290
285
280
B.E. (eV)
C_A
C_B
C_C
C_D

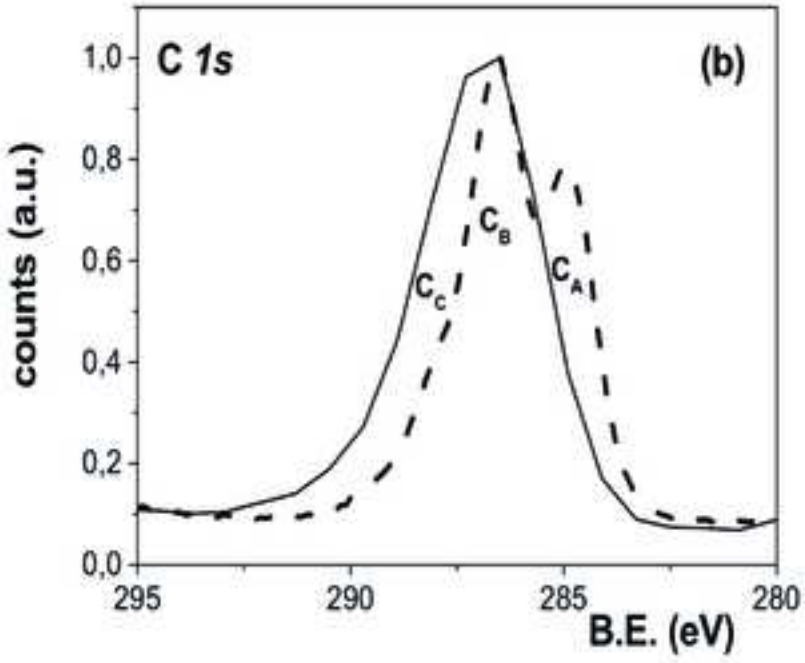
C 1s
(b)
counts (a.u.)
1,0
0,8
0,6
0,4
0,2
0,0
295
290
285
280
B.E. (eV)
C_A
C_B
C_C

Figure(s)

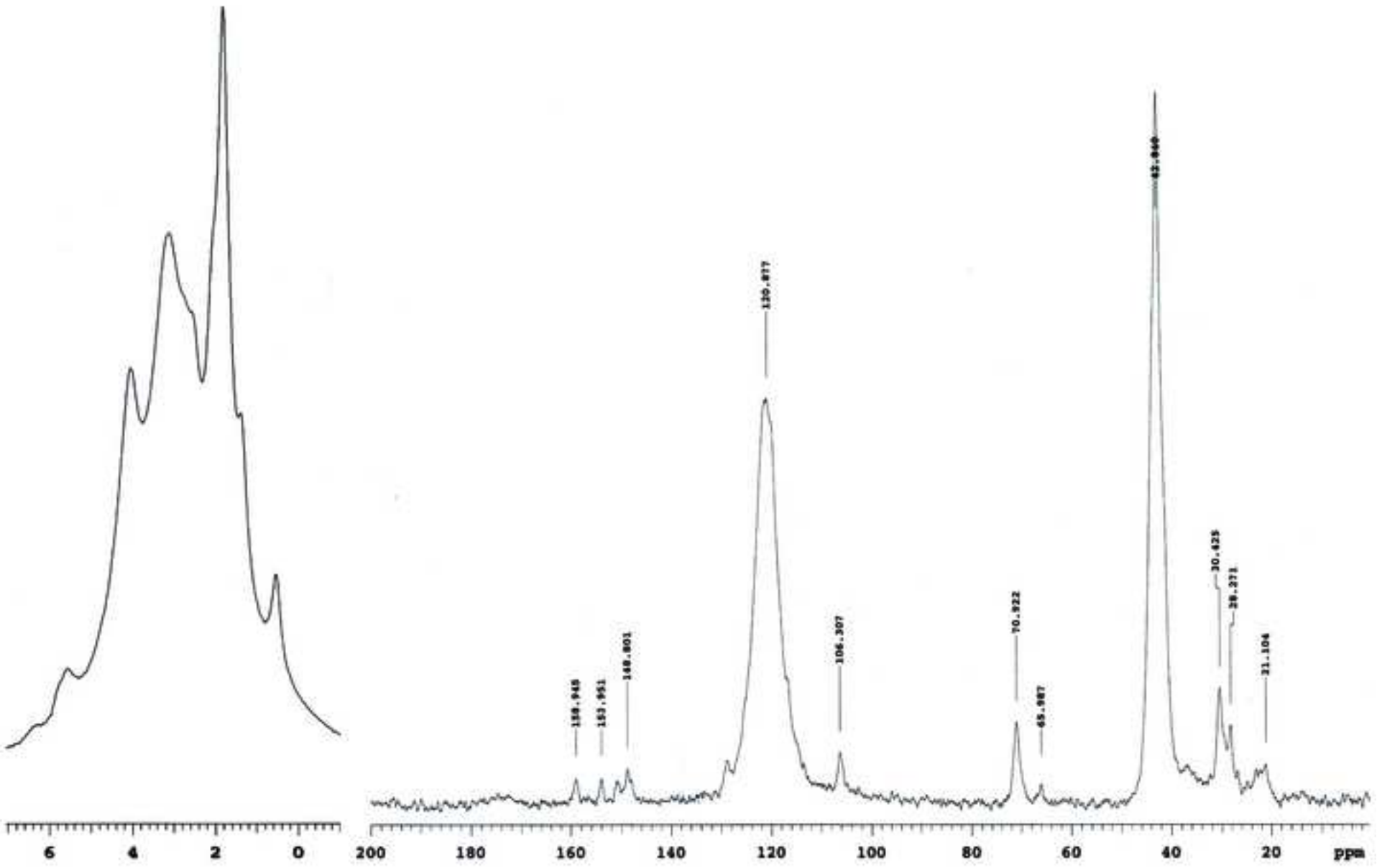
159.948
153.951
148.801
120.817
106.307
70.922
65.987
43.848
30.425
28.271
21.104
6
4
2
0
200
180
160
140
120
100
80
60
40
20
ppm

Figure(s)

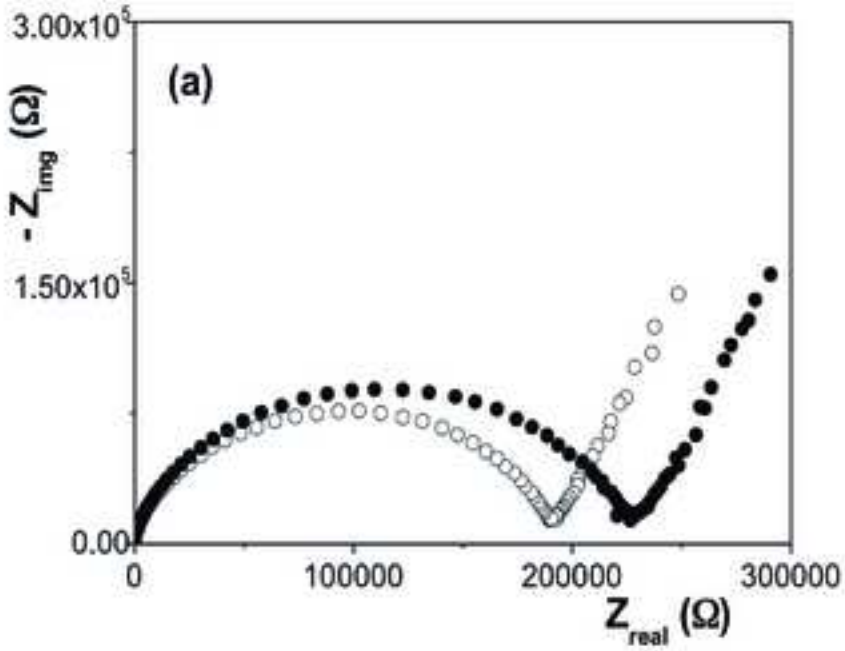
3.00x10^5
1.50x10^5
0.00
- Z_img (Ω)
(a)
0
100000
200000
300000
Z_real (Ω)

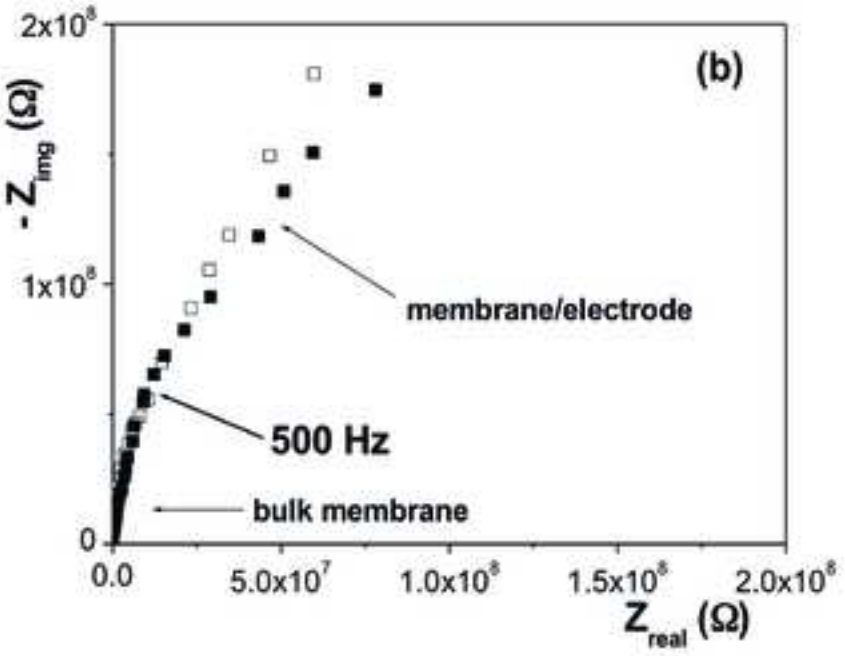
2x10^8
1x10^8
0
- Z_img (Ω)
(b)
membrane/electrode
500 Hz
bulk membrane
0.0
5.0x10^7
1.0x10^8
1.5x10^8
2.0x10^8
Z_real (Ω)

Figure(s)

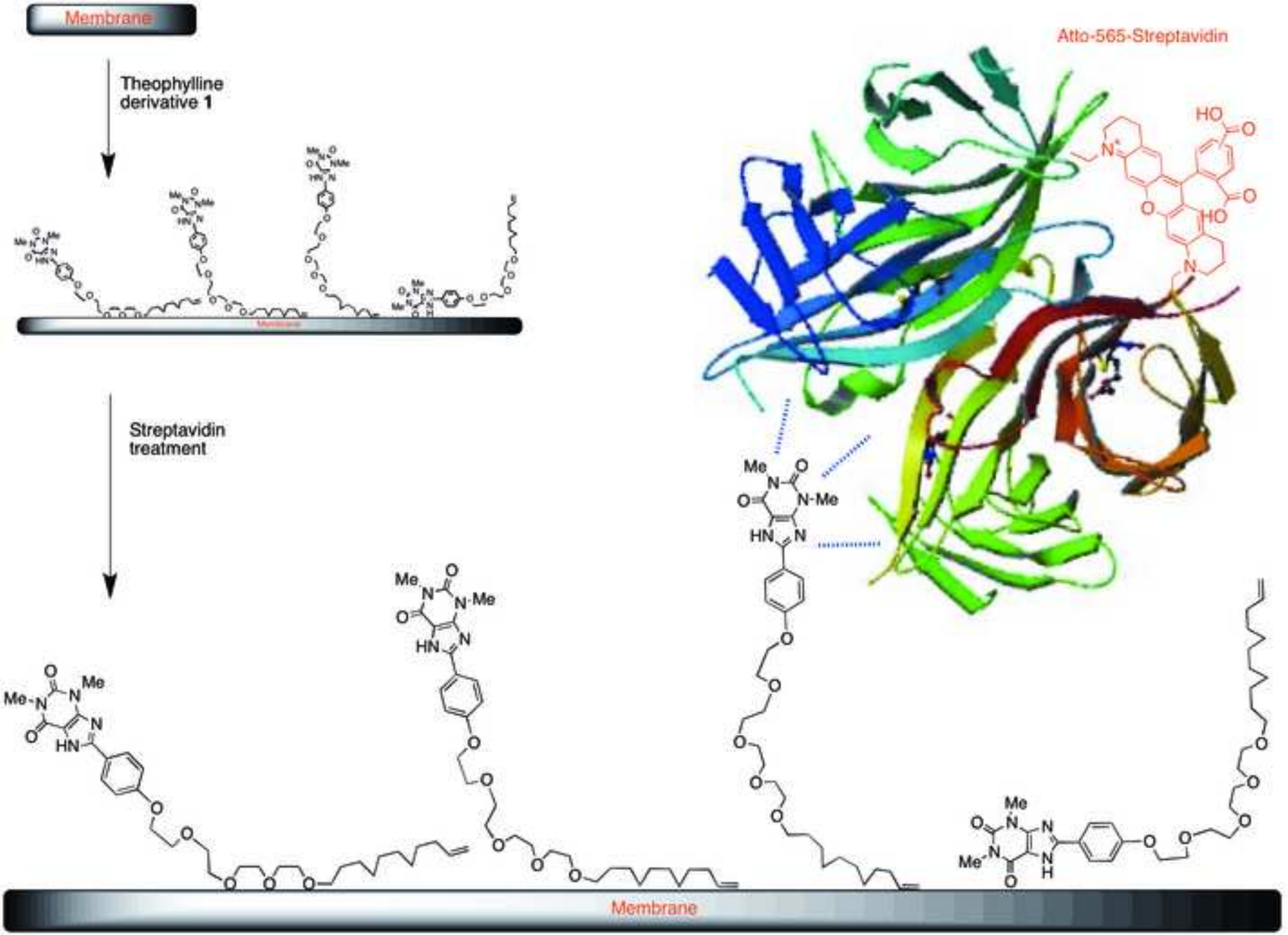
Membrane
Theophylline derivative 1
Streptavidin treatment
Atto-565-Streptavidin
Membrane

Figure(s)

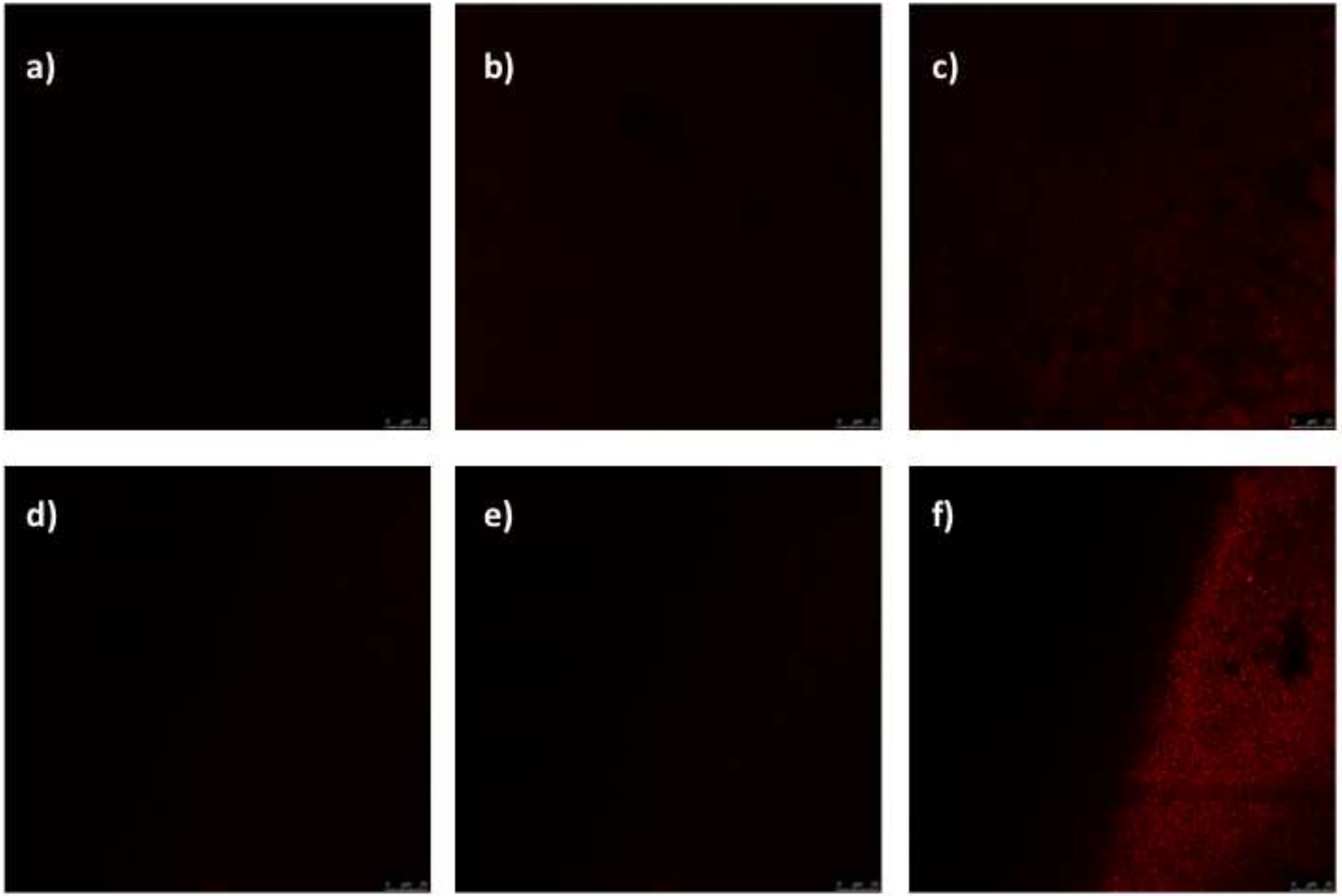

***Graphical Abstract (for review)**